Published in final edited form as:
Biomacromolecules. 2008 September ; 9(9): 2438–2446. doi:10.1021/bm800459v.

Self-Assembling Peptide-Polymer Hydrogels Designed From the Coiled Coil Region of Fibrin

Peng Jing[4], **Jai S. Rudra**[1], **Andrew B. Herr**[3], and **Joel H. Collier**[1,2,*]

[1] Department of Surgery, University of Chicago, Chicago, IL 60637

[2] Committee on Molecular Medicine, University of Chicago, Chicago, IL 60637

[3] Department of Molecular Genetics, Biochemistry, and Microbiology, University of Cincinnati College of Medicine, Cincinnati, OH 45267

[4] Department of Biomedical Engineering, University of Cincinnati, Cincinnati, OH 45221

Abstract

Biomaterials constructed from self-assembling peptides, peptide derivatives, and peptide-polymer conjugates are receiving increasing attention as defined matrices for tissue engineering, controlled therapeutic release, and in vitro cell expansion, but many are constructed from peptide structures not typically found in the human extracellular matrix. Here we report a self-assembling biomaterial constructed from a designed peptide inspired by the coiled coil domain of human fibrin, the major protein constituent of blood clots and the provisional scaffold of wound healing. Targeted substitutions were made in the residues forming the interface between coiled coil strands for a 37-amino acid peptide from human fibrinogen to stabilize the coiled coil peptide bundle, while the solvent-exposed residues were left unchanged to provide a surface similar to that of the native protein. This peptide, which self-assembled into coiled coil dimers and tetramers, was then used to produce triblock peptide-PEG-peptide bioconjugates that self-assembled into viscoelastic hydrogel biomaterials.

Keywords

Biomaterial; bioconjugate; circular dichroism; viscoelasticity; self-assembly; scaffold

INTRODUCTION

Biomaterials that are constructed from self-assembling subunits are receiving increasing attention for a number of biotechnological and biomedical applications including defined extracellular matrices for in vitro cell expansion,[1, 2] controlled release of therapeutics,[3, 4] and scaffolds for tissue engineering.[5–7] Self-assembled biomaterials possess a number of advantageous properties compared to other biomaterial scaffolds such as synthetic polymers or tissue-derived biopolymers, including complete compositional definition, the ability to produce complex fibrillar or network structures, stimulus-sensitivity, and modularity. Peptide-based self-assembling biomaterials have received particular attention owing to peptides' ease of synthesis, their ability to incorporate native or non-native chemistry, their specifiable biological activity, and the availability of design rules for producing predictably folded and

*To whom correspondence should be addressed. JHC: collier@uchicago.edu, 773-834-4161 (tel), 773-834-4546 (fax).

Supporting Information Available: MALDI *m/z* values. This information is available free of charge via the Internet at http://pubs.acs.org.

oligomerized structures. In recent years, a number of self-assembling peptide-based biomaterials have been introduced, providing novel routes towards bioactive, engineered extracellular matrices (for recent reviews, see [8–14]). The majority of these materials have been based on de novo amino acid sequences or have utilized primary structures, secondary structures, or supramolecular structures not normally found in the human extracellular matrix, including β-sheet fibrils,[2, 7, 15–21] peptide amphiphiles,[1, 6, 22] and coiled coils derived from non-human,[23–25] intracellular,[24] or de novo peptides.[23, 26–32] For in vivo applications such as tissue engineering or controlled therapeutic release, it may be advantageous to employ a synthetic self-assembled biomaterial that utilizes peptides more reminiscent of the native human extracellular matrix to reduce the risk of immunogenicity and to enhance the native functionality of these materials.

As a step towards more native self-assembled biomaterials, we describe here a peptide-polymer system derived from the coiled coil region of fibrin, the major protein constituent of the hemostatic plug and the provisional scaffold present in the early stages of wound healing (Figure 1). The folding and assembly behavior of native peptides from the coiled coil region were investigated, and amino acid substitutions were made to promote coiled coil folding and assembly. These amino acid substitutions were targeted to the residues that compose the interface between coiled coil strands, leaving the solvent-exposed residues unchanged in a strategy aimed at reducing the likelihood of immunogenicity for future *in vivo* application of these materials. In the canonical heptad $(\boldsymbol{abcdefg})_n$ repeat for coiled coil structures, residues in the ***a*** and ***d*** positions tend to be non-polar and are positioned in the hydrophobic core of coiled coil bundles. Residues in the ***e*** and ***g*** positions are likewise involved in inter-strand interactions, but through electrostatic charge pairs. Amino acids in the ***b***, ***c***, and ***f*** positions are exposed to the solvent. In the strategy reported here, the peptide $\gamma_{52–88}$KI was designed to oligomerize reliably via substitutions in ***a***, ***d***, or ***g*** residues, leaving the solvent-exposed ***b***, ***c***, and ***f*** positions intact (Figure 2). This peptide was then conjugated to polyethylene glycol (PEG) to form a triblock peptide-PEG-peptide and a diblock PEG-peptide, and the gelation behavior of these materials was investigated.

In contrast to other PEG-based block copolymers with unstructured end blocks,[33–36] coiled coils provide more specific and complementary interactions including electrostatic pairing between ***e*** and ***g*** residues and knobs-into-holes packing of the hydrophobic ***a*** and ***d*** residues. In many cases this leads to more stable and specific oligomerized structures. A number of such coiled coil-based self-assembling biomaterials have been recently described, including the peptide graft copolymers developed by Kopeček and coworkers that utilize *de novo* sequences and sequences from the drosophila kinesin stalk,[23, 24, 37] the *de novo* coiled coil proteins developed by Tirrell and coworkers, [25, 32, 38–40] and the *de novo* coiled coil PEG block copolymers developed by Klok and coworkers.[27, 28] These investigations have provided key information regarding the design of such materials, including the time-dependence of network disassembly,[25, 41] strategies for covalent stabilization of such matrices,[40] mechanisms for controlling network topography and loop formation,[25] and the ability of peptide coiled coil assembly to tolerate PEG conjugation.[28] In addition, this work has been greatly facilitated by detailed knowledge of the primary structure patterns necessary for specifying oligomerization state and orientation.[42–46] These previous studies have served as a basis for the present work, which has sought to produce synthetic self-assembling hydrogels that employ coiled coil sequences presenting solvent-exposed residues found in human fibrin.

MATERIALS AND METHODS

Peptide and PEG-peptide synthesis

Peptides (sequences in Table 1, helical wheel projections in Figure 2) were synthesized on a CS Bio 136 automated peptide synthesizer using standard Fmoc solid phase chemistry with

HOBt/HBTU activation. C-terminal amides were produced using Rink amide AM resin (NovaBiochem #01-64-0038), and the N-termini of all peptides were acetylated. Peptides were cleaved and deprotected using conventional TFA-based cleavage cocktails, and crude peptides were collected by precipitation in cold diethyl ether. For purification a Varian ProStar high performance liquid chromatography (HPLC) system was utilized (Vydac C18 column 218TP, water-acetonitrile gradient). Acetonitrile was removed via centrifugal evaporation, and peptides were stored as lyophilized powders at −20°C until further experimentation. Peptide *m/z* was assessed with electrospray ionization (ESI) or matrix-assisted laser desorption/ionization (MALDI) mass spectrometry (see Supplementary Information), and purity was assessed with analytical HPLC. For Tyr-containing peptides (all but $\beta_{110–144}$), peptide concentrations in stock solutions were verified by absorbance at 274 nm. Peptide-PEG conjugates were produced using cysteine-maleimide chemistry. Diblock PEG-γKI and triblock γKI-PEG-γKI were produced from the peptide Cys-$\gamma_{52–88}$KI and PEG$(Mal)_2$ (3.4 kDa PEG spacer, SunBio, South Korea). Prior to conjugation, any disulfides present were reduced using 4–5 equivalents of tris(2-carboxyethyl)phosphine (TCEP) in degassed phosphate buffer (100 mM phosphate/1 mM EDTA/pH 4–4.5) for 1 hr. The reduced peptide was then dialyzed against degassed phosphate buffer (pH 6.5) in a sealed container overnight to remove the TCEP. To the resultant peptide solution, two equivalents of PEG$(Mal)_2$ were added in 0.5 eq increments over the course of 24 h at pH 6.5 until the peptide peak disappeared by HPLC, indicating completion of the reaction. Diblock, triblock, and unreacted PEG were then separated on a C4 semipreparative HPLC column using an acetonitrile/water/0.1% TFA gradient elution from 40–52% acetonitrile over 35 min.

Circular Dichroism

An AVIV 215 circular dichroism spectropolarimeter was used with 0.1 cm pathlength quartz cells. Stock solutions were prepared by adding degassed Milli-Q water to lyophilized peptides, and peptide concentrations were determined by Tyr absorbance using A_{274}. Stock solutions were diluted to a working concentration of 10–100 μM in Dulbecco's phosphate buffered saline (PBS, 0.2 g/L KCl, 0.2 g/L KH_2PO_4, 8 g/L NaCl, 1.15 g/L Na_2HPO_4), and pH was adjusted using HCl or NaOH. Using the solution conditions described, adequate signal strength was observed at wavelengths greater than 195nm.

Analytical Ultracentrifugation (AUC)

To evaluate peptide oligomerization state, we utilized a Beckman XL-I analytical ultracentrifuge (Beckman Coulter, Palo Alto, CA). Prior to centrifugation, samples were dissolved in PBS and dialyzed overnight against PBS. The dialysate was utilized as the reference buffer. Sedimentation velocity experiments were performed at 48,000 rpm at 20°C. The peptide $\gamma_{52–88}$KI was analyzed at concentrations of 45 μM and 90 μM, and the program SEDFIT was used to fit the velocity data and determine continuous size distributions.[47] For the 45 μM samples, the frictional ratio was 1.768, and for the 90 μM samples, the frictional ratio was 1.784. For all samples, s_{min} was 0.1, s_{max} was 5, and the confidence level was 95%. For sedimentation equilibrium experiments, samples of $\gamma_{52–88}$KI at 46 μM and 92 μM were spun at 36,000, 40,000, and 48,000 rpm at 20° C until equilibrium was reached. Data were collected at 230 nm, trimmed using WinReedit, and analyzed globally using WinNonlin (http://www.rasmb.bbri.org/) as described.[48] The data were fitted by a number of possible association schemes; the best fit corresponded to a dimer-tetramer equilibrium. The association equilibrium constant in absorbance units reported by WinNonlin was converted to molar units as described.[49]

Peptide Cytotoxicity

A standard 3-(4,5-dimethylthiazol-2-yl)-5-(3-carboxymethoxyphenyl)-2-(4-sulfophenyl)-2H-tetrazolium (MTS) assay was utilized to determine peptide cytotoxicity (Promega, Madison, WI, cat# G3582). Primary human umbilical vein endothelial cells (HUVECs) were purchased from Lonza (Basel, Switzerland), seeded at a density of 8,850 cells/cm^2 in 96-well plates, cultured to confluence over three days in endothelial cell growth medium-2 (EGM-2, Lonza, Basel, Switzerland), and then incubated in EGM-2 containing 0.01–1.0mg/mL peptide for 24h. After incubation with peptides, the medium was replaced, MTS reagent was applied for 4h, and absorbance at 490nm was measured using a microplate reader. Controls included cultures without peptide and cultures that were fixed with absolute ethanol.

SDS-PAGE and Mass Spectrometry

Peptide samples were mixed 1:1 with SDS-PAGE sample buffer (2% SDS, 40% glycerol, 0.25 mg/mL bromophenol blue in 200 mM Tris buffer, pH 6.8) and electrophoresed on 10–20% Tris-tricine gels (Biorad). Gels were fixed with 40% methanol and stained with Coomassie Brilliant Blue R250. To label PEG products, the gels were incubated with 5% $BaCl_2$ for 10 min, rinsed with water, stained with 0.1 M iodine for 10 min, and rinsed.[50] For ESI-MS, peptides were dissolved in 50% ACN/H_2O/0.1% folic acid and injected into a Micromass Q-TOF II mass spectrometer (Waters) using a syringe pump. The acquired data were processed using MassLynx 4.0 software. MALDI was performed on a Bruker Biflex III instrument using α-cyano-4-hydroxycinnamic acid as the matrix. Positive ions were analyzed in linear mode.

Viscoelasticity measurement

Viscoelasticity was measured using a Bohlin Gemini rheometer (Malvern Instruments, Worcestershire, UK). Peptides were dissolved in water at the indicated concentration. Sonication and vortexing enabled the formation of homogeneous gel samples, and 80 μL of the material was transferred to the bottom plate of the rheometer. The upper plate (parallel plate, 8mm diameter) was lowered until it was in conformal contact with the top surface of the material, corresponding to gap distances of about 1.5 mm. Storage and loss moduli were measured at 0.1% strain and at oscillating frequencies between 0.01 and 10 Hz. The temperature was maintained at 25°C, and a humidified chamber was used to prevent evaporation.

Gel degradation

Peptide-polymers were dissolved in 5mM sodium phosphate/20 mM NaCl/pH 7.4 at a concentration of 8 wt %, vortexed, and sonicated to produce independent and homogeneous 100 μL gels. These gels were lightly centrifuged to the bottom of flip-top polypropylene tubes (mini-centrifuge, 1000 rpm for 60 seconds) to produce samples with consistent volumes and surface areas for dissolution studies. To measure gel dissolution in excess solvent, these gels were overlaid with ten additional volumes of PBS, and dissolved peptide was monitored in the supernatant over 12 days through Tyr absorbance at 274 nm. For each measurement, 300 μL of supernatant was transferred to a cuvette, measured, and carefully replaced back over the sample. A small amount of supernatant volume was lost with each measurement owing to the transfer process, and this was accounted for in the absorbance readings. Triblock gels were measured in triplicate and included samples from two different synthetic batches. Results were expressed as % dissolution with respect to plateau concentrations of dissolved peptide, and a single sample of 8 wt % diblock PEG-γKI, which dissolved immediately, was analyzed for comparison. A small amount of insoluble material remained after equilibrium had been reached with the triblock. This material was collected by centrifugation, dried under vacuum, and weighed.

Statistical Analysis

Cytotoxicity experiments contained six replicates, and statistical significance was determined using ANOVA with Tukey's HSD post-hoc comparisons.

RESULTS AND DISCUSSION

Peptide Design

The peptide $\gamma_{52–88}$KI, which assembled into α-helical coiled coil bundles (Figure 3), was designed through a series of steps starting with the coiled coil region of human fibrin. Sequences of investigated peptides are given in Table 1, and helical wheel projections are shown in Figure 2. Fibrin is the major protein constituent of blood clots and is a significant component of the provisional extracellular matrix involved in wound healing. Fibrin and its precursor, fibrinogen, are dimers of trimers, with each trimer being composed of an α, β, and γ chain. In the whole protein of fibrin(ogen), two of these trimers are joined together to form a symmetric dimer via a disulfide knot in the central globular domain, where the N-termini of all six chains are clustered (Figure 1a). Fibrin(ogen)'s coiled coils are three-chain parallel superhelices, 112 residues long, bounded by the central disulfide knot at their N-termini and another disulfide knot at their C-termini. To identify short synthetic peptides from these regions with a propensity to oligomerize into coiled coils, the coiled coil prediction tool MULTICOIL[51] was employed as a first step. Three series of overlapping 35-amino acid peptides spanning the coiled coil regions of each of the α, β, and γ chains were evaluated. In well-designed coiled coils, this peptide length represents a reasonable trade-off between stability and ease of synthesis.[52] There were four main regions in human fibrin where the corresponding 35-aa peptides were predicted to form coiled coils: near the C-terminal disulfide knot in the α-chain, in the central region of the coiled coil in the β-chain, and near both the N-terminal and C-terminal disulfide knots in the γ-chain (Figure 4). Notably, in no common region were peptides from all three chains predicted to have high coiled coil-forming propensities. This was further supported by the random coil secondary structure observed by CD for the native fibrin peptides $\alpha_{68–102}$, $\beta_{110–144}$, and $\gamma_{49–83}$, all taken from the same region immediately downstream of the N-terminal disulfide knot (data in Figure 5a, peptides correspond to the circled area in Figure 1a). Both single-peptide solutions and mixtures of all three peptides formed indistinguishable random coil secondary structures, which was not surprising given the significant number of polar residues that occupy ***a*** or ***d*** positions in these native peptides (helical wheel projection in Figure 2a). In the protein, these buried polar residues can be accommodated by the stabilizing effects of the two terminal disulfide knots and by the coiled coil's long length, but these factors are absent in short peptide systems. Collectively, these initial investigations illustrated that the construction of heterotrimers based on all three chains would be challenging, most likely involving many amino acid substitutions, difficult syntheses of long peptides, and the covalent conjugation of two or more different chains together via partial or complete reconstruction of one of the disulfide knots. While this would be possible, we elected to design homooligomeric parallel multimers from the most promising short sequences of the fibrin coiled coil as a more efficient approach.

For homooligomeric coiled coil construction, the N-terminus of the γ chain was selected owing to its high score in MULTICOIL, its having few polar residues buried in the hydrophobic core, and because residues in its ***e*** and ***g*** positions could form two productive electrostatic interactions in homooligomeric parallel bundles with only one substitution. Although peptides from the C-terminal region of the γ chain also had high MULTICOIL scores, the folding of this region is complicated in human fibrin by the presence of an antiparallel fourth helix from the C-terminus of the α-chain.[53] To improve the coiled coil forming ability of $\gamma_{49–83}$, three amino acid substitutions were made to produce $\gamma_{49–83}$QQK. The replacement of the N-terminal Cys_{49} and the conformationally flexible Gly_{50} was intended to improve the helical propensity of the N-

terminus, and the replacement of Asp_{65} with Lys was intended to change a destabilizing Asp-Asp charge pair between ***e*** and ***g*** residues into a coiled coil-stabilizing Lys-Asp charge pair. It was found that $\gamma_{49–83}$QQK demonstrated improved helical character in acidic conditions, but this was not an improvement over the native peptide $\gamma_{49–83}$, which also demonstrated this behavior at low pH (Figure 5b). Additionally, at neutral pH, the CD spectrum of $\gamma_{49–83}$QQK continued to show significant random coil character. One explanation for the loss of helicity at neutral pH was that the isoelectric points of both $\gamma_{49–83}$ and $\gamma_{49–83}$QQK were acidic (~4.2 and 4.9, respectively). Moreover, both peptides possessed two polar residues in the putative ***a*** and ***d*** residues of their heptad repeats, further destabilizing coiled coil folding.

In order to provide a peptide with a neutral isoelectric point and no buried polar residues, peptide $\gamma_{52–88}$KI was produced by substituting all ***a*** and ***d*** residues with isoleucine, shifting the sequence C-terminally by three amino acids, and lengthening the sequence by two amino acids to provide a peptide with no buried polar residues, two complementary electrostatic interactions between ***e*** and ***g*** residues in parallel bundles, and a neutral isoelectric point (~6.7). No amino acids in the putative ***b***, ***c***, ***e***, or ***f*** positions were substituted in this peptide, and only one substitution was made in a ***g*** position, a strategy designed to maintain the hydrated residues of the native fibrin peptide in order to minimize the risk of immunogenicity for future *in vivo* work. This peptide was the end result of the design process outlined above, and it served as the basis for constructing the biomaterials reported in the rest of this paper.

Folding and oligomerization behavior of $\gamma_{52–88}$KI

The peptide $\gamma_{52–88}$KI formed helical secondary structures in aqueous solutions (Figure 3a–b). CD spectra of this peptide displayed prominent minima at 208 nm and 222 nm characteristic of α-helical folding, and the ellipticity ratio of $[\theta]_{222}/[\theta]_{208}$ for this peptide strongly suggested coiled coil oligomerization. Previous studies have found values of this molar ellipticity ratio to be in the range of about 1.02 to 1.1 for coiled coils, with values somewhat smaller for monomeric α-helices.[24, 54, 55] The peptide $\gamma_{52–88}$KI demonstrated a $[\theta]_{222}/[\theta]_{208}$ ellipticity ratio of 1.06, suggesting that it oligomerized into coiled coils. The secondary structure of $\gamma_{52–88}$KI did not change significantly within a pH range between pH 4 and pH 7 (Figure 3a), and it was also unchanged in a range of concentrations from 100 μM to as low as 10 μM (Figure 3b). This indicated that the coiled coil structure was stable in a range of pH and did not dissociate or denature upon dilution. Although $\gamma_{52–88}$KI demonstrated CD spectra indicating predominantly helical character, the magnitudes of the ellipticities at 208 nm and 222 nm were somewhat smaller than those expected for a 100% helical peptide. To clarify whether this might be attributable to the presence of a fraction of random coil peptides, the oligomerization behavior of $\gamma_{52–88}$KI was investigated with analytical ultracentrifugation. Sedimentation velocity experiments were performed on 45 μM and 90 μM peptide in PBS, and it was found that $\gamma_{52–88}$KI sedimented as a mixture of two species with estimated molecular weights close to dimers and tetramers (Figure 3c). Subsequent sedimentation equilibrium analysis confirmed that $\gamma_{52–88}$KI existed in a dimer-tetramer equilibrium (Figure 3d), with a dissociation constant of 4.95 μM (dimer concentration units). These experiments indicated that the slightly reduced ellipticities observed by CD were most likely not attributable to the presence of monomeric random coil peptides but to portions of the oligomerized bundles that were not 100% helical, most likely the peptide termini. It was anticipated that $\gamma_{52–88}$KI would form trimers rather than dimers and tetramers, given the trimeric nature of the native fibrin coiled coil and the all-isoleucine hydrophobic core of $\gamma_{52–88}$KI, which would also be expected to favor trimerization,[56] but previous reports have also found oligomerization state to change for other peptides when taken out of the context of their native proteins.[23] It may also be possible that the unmodified ***b***, ***c***, or ***f*** residues played a role in specifying oligomerization state.[57, 58] Although not expected, the dimer-tetramer oligomerization behavior of $\gamma_{52–88}$KI was fortuitous for the subsequent construction of hydrogels from this peptide, as tetrameric assemblies can serve as more highly

substituted cross-link points than trimeric cross-link points. It is not known whether the dimers and tetramers observed are in a parallel arrangement or an antiparallel arrangement, but the charged residues in the ***e*** and ***g*** positions would be expected to strongly favor a parallel arrangement.

Neither $\gamma_{52–88}$KI nor $\gamma_{49–83}$QQK was cytotoxic to primary human endothelial cells (Figure 6). This evaluation was undertaken at this stage to exclude the possibility that the amphiphilic peptides could compromise the integrity of the cell membrane or be otherwise cytotoxic. These materials are intended for use as chemically defined cell culture matrices or scaffolds for regenerative medicine, so understanding this aspect at the early stages of their design is important. Collectively, the strongly α-helical CD spectra of $\gamma_{52–88}$KI, its stability in a range of pH and concentrations, its oligomerization into dimers and tetramers by AUC, and its non-cytotoxicity indicated that this peptide was an excellent candidate as a self-assembling element for synthetic hydrogel biomaterials.

Behavior of diblock and triblock $\gamma_{52–88}$KI PEG-peptides

Cysteine-$\gamma_{52–88}$KI was synthesized and conjugated to dimaleimido-PEG having an average molecular weight of 3,400 Da. Mixtures of diblock (PEG-γKI) and triblock (γKI-PEG-γKI) were produced and separated by semi-preparative reverse-phase HPLC. Yields of the peptide conjugation reactions were acceptable, as 24%–41% of the peptide was recovered as purified triblock, and 15%–27% of the peptide was recovered as purified diblock, depending on the synthesis run. In all, 51%–56% of the peptide was recovered as purified peptide-polymers. SDS-PAGE of the diblock and triblock revealed expected molecular weights and staining patterns with Coomassie and iodine stains, where $BaCl_2$ and iodine react with the PEG chains to produce a brown color (Figure 7c). In addition, the identity and purity of the diblock and triblock were verified with ESI-MS (Figure 7a–b), which also exhibited 44 Da mass differences between discrete polymer chains reflective of one ethylene glycol monomer unit, which arose from the polydisperse dimaleimido-PEG.

PEG conjugation had only a small impact on the secondary structure of $\gamma_{52–88}$KI, as both the diblock and triblock retained their coiled coil character (Figure 8, Table 2). The CD spectra of both PEG-γKI and γKI-PEG-γKI displayed prominent minima at 208 nm and 222 nm, and their $[\theta]_{222}$ values were only slightly reduced compared with $\gamma_{52–88}$KI. In addition, the $[\theta]_{222}/[\theta]_{208}$ ellipticity ratios decreased only slightly from 1.06 to 1.03 for both the diblock and the triblock PEG-peptides (Table 2). Also, like the unconjugated $\gamma_{52–88}$KI peptide, the secondary structures of the diblock and triblock were stable even when diluted to as low as 10 μM. These results indicated that $\gamma_{52–88}$KI retained its ability to form coiled coil structures when conjugated to PEG in a diblock or triblock configuration at the peptides' N-terminus.

Both PEG-γKI and γKI-PEG-γKI were highly soluble in water, but the viscoelastic properties of their solutions differed dramatically. When diblock PEG-γKI was dissolved in phosphate buffer, it formed non-viscous solutions even at concentrations as high as 12 wt %. In stark contrast, triblock γKI-PEG-γKI formed transparent and elastic hydrogels. Whereas even 12 wt % solutions of the diblock could be easily pipetted, the triblock solutions formed self-supporting elastic materials that could not be pipetted and could be manipulated as solids. Using oscillating rheometry to quantify the viscoelastic properties of the materials, it was found that γKI-PEG-γKI hydrogels possessed storage moduli (G′) of about 2.5 kPa at 1 Hz for 12 wt % hydrogels and about 600 Pa at 1 Hz for 8 wt % hydrogels (Figure 9a). For both concentrations, storage moduli were significantly greater than loss moduli, and no crossings of G′ and G″ were observed in the frequency range tested. The loss modulus (G″) was about 200 Pa for 12 wt % gels and 100 Pa for 8 wt % gels at 1 Hz, corresponding to tan δ values of 0.08 for 12 wt % gels and 0.16 for 8 wt % gels. Gels at both concentrations demonstrated some frequency sensitivity in storage and loss moduli between 0.01–10 Hz, but these differences were small, especially

for 12 wt % gels. In comparison with other PEG-based triblock copolymers with unstructured hydrophobic end blocks such as fluorocarbons,[36] the triblock γKI-PEG-γKI exhibited much less frequency sensitivity, indicating that the cross-links provided by the oligomerized peptides were significantly less dynamic than for purely polymeric block copolymers. Collectively, this relative frequency insensitivity, G′ values around 1 kPa, small tan δ values, and absence of crossings between G′ and G″ indicated that γKI-PEG-γKI formed cross-linked hydrogels. In contrast, the rheological characteristics of the diblock PEG-γKI were significantly different. The diblock demonstrated significantly lower storage moduli between 0.1–10 Pa, significant frequency sensitivity, and storage and loss moduli of similar magnitudes, both at 8 wt % and at 12 wt %. It is also possible that the rheological data for the diblock contain some amount of experimental noise owing to the very low moduli of the material. This contrasting behavior between the triblock and diblock PEG-peptides suggests that the mechanism of gelation of γKI-PEG-γKI is as proposed in Figure 1c, that is through the cross-linking of PEG chains by the coiled coil domains. Had the mode of gelation been predominantly through physical entanglement of distinct micelles or small supramolecular aggregates, it would be expected that the rheological characteristics of the diblock and triblock would be more similar. Moreover, a micellar packing mode of gelation would also be expected to produce materials that would rapidly dissociate when incubated in excess solvent. To investigate this aspect, we compared the dissolution of gels of 8 wt % diblock PEG-γKI and triblock γKI-PEG-γKI when incubated in excess PBS. The diblock PEG-γKI dissolved almost immediately, but the triblock γKI-PEG-γKI demonstrated an initial rapid dissolution of only about 30%, followed by a much slower dissolution of the remaining material over about eight days (Figure 9b). It is not known specifically why the triblock demonstrated this extended dissolution time, but it possibly arose from the low dimer-tetramer dissociation constant indicated by AUC equilibrium experiments for $\gamma_{52–88}$KI (about 5 μM). The concentration of the triblock used in the dissolution experiments was several orders higher than this dissociation constant, so slow dissolution would be expected. Additionally, 25% of the starting triblock mass remained at the end of the experiment as a poorly soluble precipitate. This result along with the initial rapid dissolution behavior may indicate that the triblock gels were composed of a heterogeneous mixture of assemblies with varying mobility and/or solubility. For example, short oligomeric loops would be expected to be more soluble initially and could have lead to the observed early dissolution, while more extensively networked oligomers may have been responsible for the slower dissolution observed between days 2 and 8. Aside from these possibilities for heterogeneity and loop formation, however, the rheometry, dissolution, AUC, and CD data collectively indicated that the conceptual model proposed in Figure 1c is generally correct.

The heterogeneity in supramolecular organization exhibited by γKI-PEG-γKI, which is a feature of self-assembling proteins and peptide-polymers,[25, 38, 41] warrants further investigation, both in terms of materials characterization and in terms of biological response. Cell interactions with such biomaterials will depend not only on the chemical nature of the constituent peptide-polymers but also on the different oligomeric species produced by their assembly. In an important approach to control this heterogeneity in network topology, Shen, Tirrell, and coworkers recently described expressed triblock proteins containing terminal coiled coil domains with differing oligomerization behaviors, thus reducing intramolecular coiled coil formation and suppressing oligomeric loop formation.[25] For the γKI-PEG-γKI gels, additional heterogeneity may also arise from polydispersity of the PEG chain, as the average molecular weight of the PEG was 3,400 Da but species with PEG chains between 2800–4000 Da were observed with mass spectrometry (Figure 7).

Although γKI-PEG-γKI self-assembles into stable hydrogels with amino acid substitutions only in putative solvent-hidden locations, it may also be possible that coiled coil sequences exist in the human extracellular matrix that do not require ***a***, ***d,*** or ***g*** position substitution as $\gamma_{52–88}$KI does. For example, Tirrell and coworkers recently reported on coiled-coil based

biomaterials employing a peptide sequence from rat cartilage oligomeric matrix protein (COMP),[25] and the human variant may be equally as useful for use as a synthetic oligomerizing domain. In addition, it is also possible that the complete substitution of all of the ***a*** and ***d*** residues in $\gamma_{52–88}$KI is not necessary for stable oligomerization. There may in fact be a peptide with an intermediate level of substitution (for example only replacing the buried polar residues of $\gamma_{52–88}$ with isoleucine) that may reliably oligomerize while conserving even more of the primary amino acid sequence than $\gamma_{52–88}$KI. Studies of how $\gamma_{52–88}$KI is tolerated immunologically will indicate whether such steps are necessary. Few self-assembling biomaterials have been extensively evaluated for their interactions with the immune system, so the relationships between primary structure, oligomerization, and immunogenicity are not well understood in the context of biomaterials. Although soluble peptides are generally not highly immunogenic, their immunogenicity can be significantly enhanced by multimerization, [59–61] fibrillization,[62] supramolecular assembly,[63] or by adjuvants that may be present at the site of delivery. One mechanism by which multimerized structures have been shown to enhance immunogenicity is through the cross-linking of B cell receptors by multivalent arrays of epitopes in a T cell-independent process, [59–61] and it is not clear to what extent self-assembled biomaterials may also engage such a response. In addition, non-native peptides may be immunogenic through phagocytosis by antigen-presenting cells such as macrophages and dendritic cells and presentation in the major histocompatibility complex (MHC) for recognition by T lymphocytes. The coiled coil materials described here provide a self-assembling strategy where the solvent-exposed residues of the coiled coil are not changed from native proteins in the ECM, thus reducing the chance for immunogenicity by T-independent B cell activation. It is still theoretically possible that the amino acid substitutions employed will be able to be recognized through phagocytosis and MHC presentation, but determination of the immunologically allowable amino acid substitutions in this system is left to a future study.

In comparison with full-length fibrin(ogen), the system reported here possesses advantageous synthetic definition, whereas fibrin(ogen) must currently be isolated from biological sources, potentially leading to batch-to-batch non-uniformity or pathogen transmission. Fibrin(ogen) is also difficult to express in culture, so fully synthetic gel-forming analogs of fibrin such as the one presented here may be a more feasible alternative to biologically sourced fibrin(ogen). Compared to heterooligomeric coiled coil hydrogels such as the ones reported by the Kopeček group, the γKI-PEG-γKI system has the advantage of only requiring the synthesis of one peptide, though the triggered gelation and more specific network topology afforded by the mixing of the complementary coiled coils is sacrificed.[31, 64] In terms of mechanical properties, the triblock molecule exhibited moduli similar to fibrin gels, although fibrin gels can attain these stiffness values at significantly lower concentrations. For example, fibrin gels typically exhibit Young's moduli of about 1 kPa at concentrations near 0.5 mg/mL and 6 kPa at concentrations near 3 mg/mL.[65] The mechanical properties of γKI-PEG-γKI gels also compare favorably with other reported hydrogels that self-assemble via homooligomeric peptides. For example, the expressed triblock proteins reported by the Tirrell group employing COMP peptides or *de novo* peptides produce hydrogels with plateau storage moduli ranging from about 500–2,000 Pa at concentrations of 7 % w/v.[25, 40, 41] These values depend primarily on the aggregation number of the oligomerized coiled coil bundles, whether covalent cross-linking strategies have been employed, and the extent to which looped chains are suppressed. In terms of the tissue engineering applications for which such hydrogels could be utilized, this range of stiffness matches relatively soft tissues such as nervous tissue, liver, and kidney.[66, 67] Collectively, the non-cytotoxicity, predictable oligomerization, and native solvent-exposed residues of $\gamma_{52–88}$KI along with the synthetic definition, gelation behavior, and attractive mechanical properties of γKI-PEG-γKI enable further exploration of these materials in biomedical technologies such as scaffolds for regenerative medicine.

CONCLUSIONS

Synthetic peptide-polymer gels that self-assemble via amino acid sequences inspired by fibrin's coiled coil domains were designed. A 37 aa peptide was produced with eleven substitutions in ***a*** or ***d*** positions and one substitution in a ***g*** position, and this peptide formed stable coiled coil dimers and tetramers, as shown by circular dichroism and analytical ultracentrifugation. This peptide, $\gamma_{52–88}$KI, was non-cytotoxic in cultures of human endothelial cells. Conjugation of this peptide to polyethylene glycol via maleimide-thiol chemistry produced self-assembling diblock and triblock molecules. PEG conjugation had a negligible impact on the secondary structure of the peptide, both for the diblock and triblock. The triblock exhibited rheologial characteristics of a cross-linked gel and had attractive mechanical properties, as the average storage modulus of 8% w/v triblock gels at 1 Hz was 600 Pa and that of 12% w/v gels was 2.5 kPa. In contrast, the diblock did not form gels even at concentrations as high as 12% w/v. The triblock gels slowly dissolved in excess phosphate buffered saline by about 50% after 2.5 days and entirely by about 8 days. Collectively, these results indicate that the triblock peptide-PEG-peptide forms hydrogels that are promising candidates for further evaluation as self-assembling biomaterials.

Supplementary Material

Refer to Web version on PubMed Central for supplementary material.

Acknowledgments

The authors thank Dale Schaeffer for access to the rheometer, Deb Conrady for help with analytical ultracentrifugation, Stephen Macha for assistance with mass spectrometry, and Paul Rosevear and Jack Howarth for access to the circular dichroism instrument. The project described was supported by Grant Number R21DE017703 from the National Institute of Dental and Craniofacial Research. The content is solely the responsibility of the authors and does not necessarily represent the official views of the National Institute of Dental and Craniofacial Research or the National Institutes of Health.

References

1. Beniash E, Hartgerink JD, Storrie H, Stendahl JC, Stupp SI. Acta Biomater 2005;1:387–397. [PubMed: 16701820]
2. Kretsinger JK, Haines LA, Ozbas B, Pochan DJ, Schneider JP. Biomaterials 2005;26:5177–86. [PubMed: 15792545]
3. Law B, Weissleder R, Tung CH. Biomacromolecules 2006;7:1261–5. [PubMed: 16602747]
4. Ramachandran S, Yu YB. Bio Drugs 2006;20:263–9.
5. Kisiday J, Jin M, Kurz B, Hung H, Semino C, Zhang S, Grodzinsky AJ. Proc Natl Acad Sci USA 2002;99:9996–10001. [PubMed: 12119393]
6. Silva GA, Czeisler C, Niece KL, Beniash E, Harrington DA, Kessler JA, Stupp SI. Science 2004;303:1352–1355. [PubMed: 14739465]
7. Jung JP, Jones JL, Cronier SA, Collier JH. Biomaterials 2008;29:2143–2151. [PubMed: 18261790]
8. Rajagopal K, Schneider JP. Curr Opin Struct Biol 2004;14:480–486. [PubMed: 15313243]
9. Mart RJ, Osborne RD, Stevens MM, Ulijn RV. Soft Matter 2006;2:822–835.
10. Dankers PYW, Meijer EW. Bull Chem Soc Jpn 2007;80:2047–2073.
11. Woolfson DN, Ryadnov MG. Curr Opin Chem Biol 2006;10:559–567. [PubMed: 17030003]
12. MacPhee CE, Woolfson DN. Curr Opin Solid State & Mater Sci 2004;8:141–149.
13. Lim YB, Lee M. J Mater Chem 2008;18:723–727.
14. Channon K, MacPhee CE. Soft Matter 2008;4:647–652.
15. Genove E, Shen C, Zhang S, Semino CE. Biomaterials 2005;26:3341–51. [PubMed: 15603830]
16. Gelain F, Bottai D, Vescovi A, Zhang S. PLoS ONE 2006;1:e119. [PubMed: 17205123]

17. Collier JH, Hu BH, Ruberti JW, Zhang J, Shum P, Thompson DH, Messersmith PB. J Am Chem Soc 2001;123:9463–9464. [PubMed: 11562238]
18. Collier JH, Messersmith PB. Bioconjugate Chem 2003;14:748–755.
19. Holmes TC, de Lacalle S, Su X, Liu G, Rich A, Zhang S. Proc Natl Acad Sci USA 2000;97:6728–33. [PubMed: 10841570]
20. Haines-Butterick L, Rajagopal K, Branco M, Salick D, Rughani R, Pilarz M, Lamm MS, Pochan DJ, Schneider JP. Proc Natl Acad Sci USA 2007;104:7791–7796. [PubMed: 17470802]
21. Schneider JP, Pochan DJ, Ozbas B, Rajagopal K, Pakstis L, Kretsinger J. J Am Chem Soc 2002;124:15030–15037. [PubMed: 12475347]
22. Guler MO, Hsu L, Soukasene S, Harrington DA, Hulvat JF, Stupp SI. Biomacromolecules 2006;7:1855–1863. [PubMed: 16768407]
23. Wang C, Stewart RJ, Kopeček J. Nature 1999;397:417–20. [PubMed: 9989405]
24. Wang C, Kopeček J, Stewart RJ. Biomacromolecules 2001;2:912–20. [PubMed: 11710049]
25. Shen W, Zhang KC, Kornfield JA, Tirrell DA. Nat Mater 2006;5:153–158. [PubMed: 16444261]
26. Mi L, Fischer S, Chung B, Sundelacruz S, Harden JL. Biomacromolecules 2006;7:38–47. [PubMed: 16398496]
27. Vandermeulen GWM, Tziatzios C, Duncan R, Klok HA. Macromolecules 2005;38:761–769.
28. Vandermeulen GWM, Tziatzios C, Klok HA. Macromolecules 2003;36:4107–4114.
29. Ryadnov MG, Woolfson DN. Nat Mater 2003;2:329–332. [PubMed: 12704382]
30. Ryadnov MG, Woolfson DN. J Am Chem Soc 2004;126:7454–5. [PubMed: 15198588]
31. Yang JY, Xu CY, Wang C, Kopeček J. Biomacromolecules 2006;7:1187–1195. [PubMed: 16602737]
32. Petka WA, Harden JL, McGrath KP, Wirtz D, Tirrell DA. Science 1998;281:389–392. [PubMed: 9665877]
33. Alexandridis P. Curr Opin Colloid Interface Sci 1997;2:478–489.
34. Mortensen K. Curr Opin Colloid Interface Sci 1998;3:12–19.
35. Mortensen K. Macromolecules 1997;30:503–507.
36. Xu B, Li L, Yekta A, Masoumi Z, Kanagalingam S, Winnik MA, Zhang KW, Macdonald PM. Langmuir 1997;13:2447–2456.
37. Yang JY, Xu CY, Kopeckova P, Kopeček J. Macromol Biosci 2006;6:201–209. [PubMed: 16514591]
38. Shen W, Kornfield JA, Tirrell DA. Soft Matter 2007;3:99–107.
39. Kennedy SB, Littrell K, Thiyagarajan P, Tirrell DA, Russell TP. Macromolecules 2005;38:7470–7475.
40. Shen W, Lammertink RGH, Sakata JK, Kornfield JA, Tirrell DA. Macromolecules 2005;38:3909–3916.
41. Shen W, Kornfield JA, Tirrell DA. Macromolecules 2007;40:689–692.
42. Oakley MG, Kim PS. Biochemistry 1998;37:12603–12610. [PubMed: 9730833]
43. Gonzalez L Jr, Woolfson DN, Alber T. Nat Struct Biol 1996;3:1011–8. [PubMed: 8946854]
44. Nautiyal S, Woolfson DN, King DS, Alber T. Biochemistry 1995;34:11645–51. [PubMed: 7547896]
45. Harbury PB, Zhang T, Kim PS, Alber T. Science 1993;262:1401–1407. [PubMed: 8248779]
46. Lumb KJ, Kim PS. Biochemistry 1995;34:8642–8648. [PubMed: 7612604]
47. Schuck P. Biophys J 2000;78:1606–1619. [PubMed: 10692345]
48. Herr AB, White CL, Milburn C, Wu C, Bjorkman PJ. J Mol Biol 2003;327:645–657. [PubMed: 12634059]
49. Herr AB, Ornitz DM, Sasisekharan R, Venkataraman G, Waksman G. J Biol Chem 1997;272:16382–16389. [PubMed: 9195945]
50. Zimmerman SB, Murphy LD. Anal Biochem 1996;234:190–193. [PubMed: 8714597]
51. Wolf E, Kim PS, Berger B. Protein Sci 1997;6:1179–1189. [PubMed: 9194178]
52. Su JY, Hodges RS, Kay CM. Biochemistry 1994;33:15501–10. [PubMed: 7803412]
53. Doolittle RF. J Thromb Haemost 2003;1:1559–65. [PubMed: 12871291]
54. Pechar M, Kopeckova P, Joss L, Kopeček J. Macromol Biosci 2002;2:199–206.

55. Graddis TJ, Myszka DG, Chaiken IM. Biochemistry 1993;32:12664–12671. [PubMed: 8251485]
56. Harbury PB, Kim PS, Alber T. Nature 1994;371:80–83. [PubMed: 8072533]
57. Papapostolou D, Smith AM, Atkins EDT, Oliver SJ, Ryadnov MG, Serpell LC, Woolfson DN. Proc Natl Acad Sci USA 2007;104:10853–10858. [PubMed: 17567757]
58. Smith AM, Banwell EF, Edwards WR, Pandya MJ, Woolfson DN. Adv Funct Mater 2006;16:1022–1030.
59. Bachmann MF, Rohrer UH, Kundig TM, Burki K, Hengartner H, Zinkernagel RM. Science 1993;262:1448–1451. [PubMed: 8248784]
60. Fehr T, Bachmann MF, Bucher E, Kalinke U, DiPadova F, Lang AB, Hengartner H, Zinkernagel RM. J Exp Med 1997;185:1785–1792. [PubMed: 9151704]
61. Rosenberg AS. AAPS J 2006;8:E501–E507. [PubMed: 17025268]
62. Maas C, Hermeling S, Bouma B, Jiskoot W, Gebbink MFBG. J Biol Chem 2007;282:2229–2236. [PubMed: 17135263]
63. Boato F, Thomas RM, Ghasparian A, Freund-Renard A, Moehle K, Robinson JA. Angew Chem Int Ed 2007;46:9015–9018.
64. Yang J, Wu K, Konak C, Kopeček J. Biomacromolecules 2008;9:510–7. [PubMed: 18208316]
65. Benkherourou M, Gumery PY, Tranqui L, Tracqui P. IEEE Trans Biomed Eng 2000;47:1465–75. [PubMed: 11077740]
66. Engler AJ, Sen S, Sweeney HL, Discher DE. Cell 2006;126:677–89. [PubMed: 16923388]
67. Levental I, Georges PC, Janmey PA. Soft Matter 2007;3:299–306.

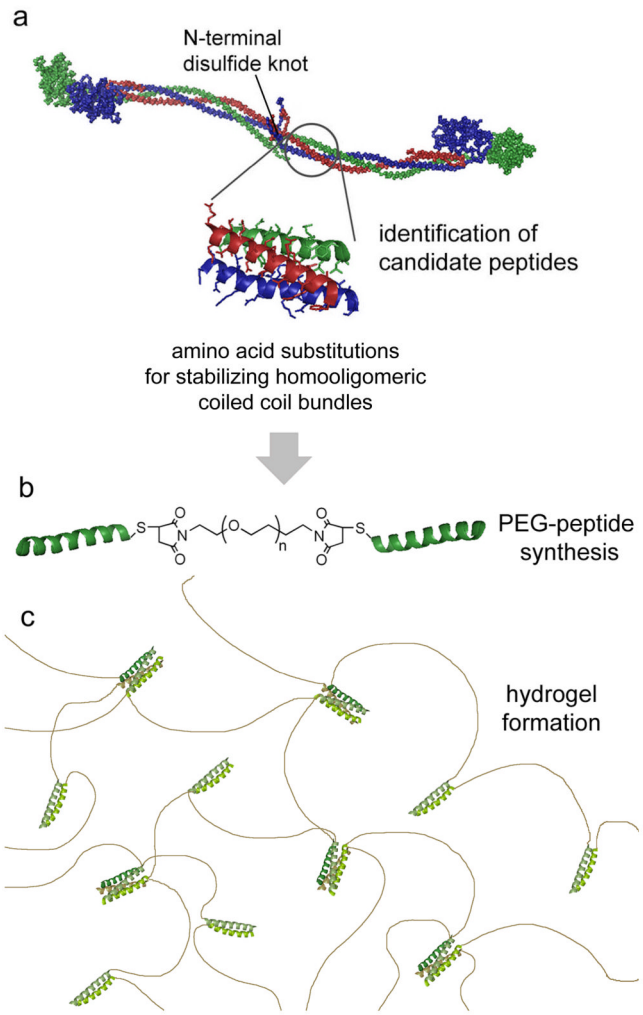

Figure 1.

Schematic for fibrin-inspired coiled coil biomaterials. Short peptides from the coiled coil domain of fibrin are identified (a, note: chicken fibrinogen is shown here owing to its elucidated crystal structure; α chain (red), β chain (blue) γ chain (green); drawing produced with PyMOL[58] from PDB ID 1EI3). Substitutions are made to stabilize homooligomeric coiled coil formation, and designed peptides are conjugated to short polyethylene glycol chains to form triblock peptide-PEG-peptides (b). Triblock copolymers self-assemble in appropriate buffers to produce hydrogels (c). Dimeric and tetrameric bundles are shown, as indicated by analytical ultracentrifugation.

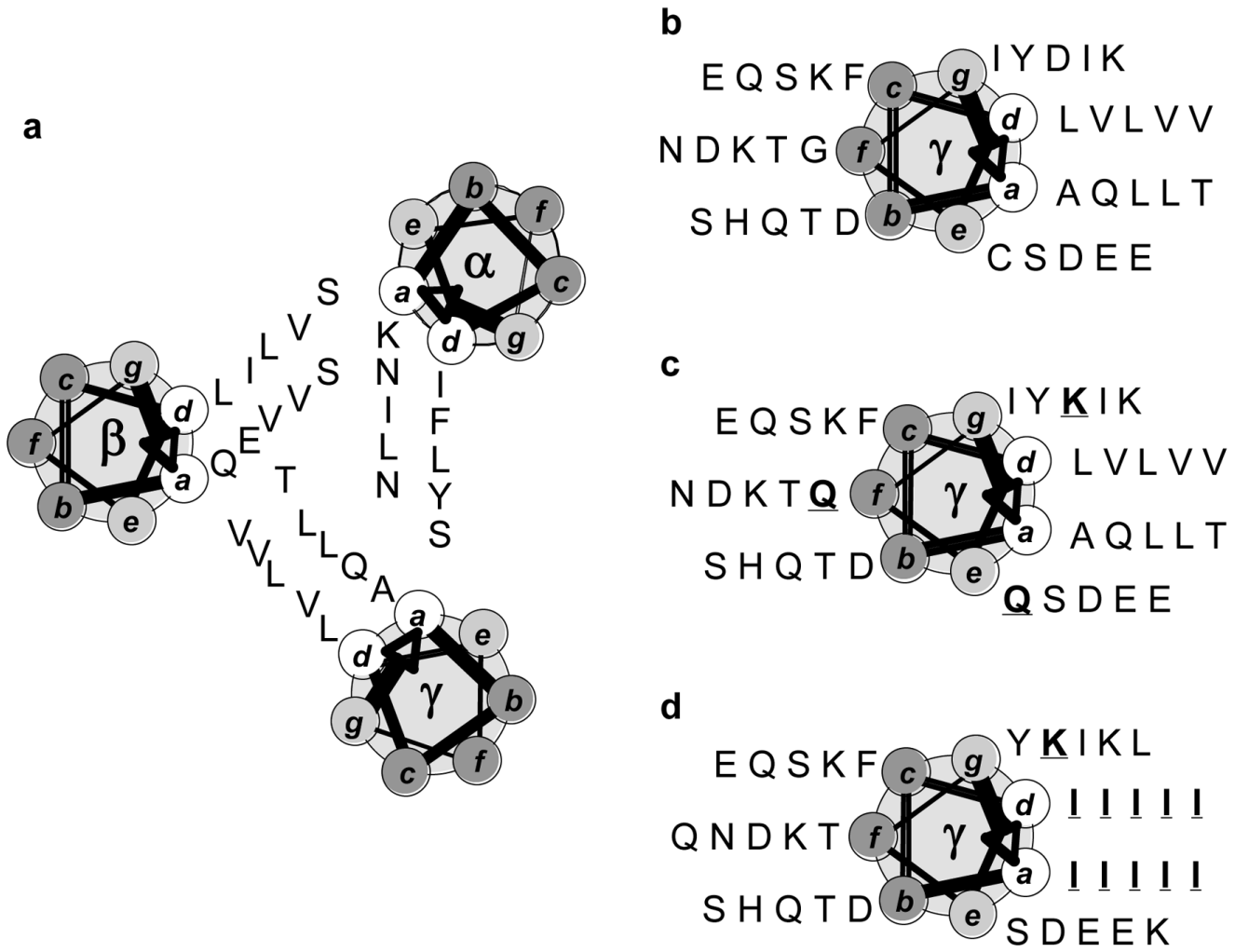

Figure 2.

N-terminal helical wheel projections showing the ***a*** and ***d*** residues for the native fibrin trimer $\alpha_{68–102}$, $\beta_{110–144}$, and $\gamma_{49–83}$, near the N-terminus of the coiled coil (a), and full helical wheel projections for $\gamma_{49–83}$, (b), $\gamma_{49–83}$QQK (c), and $\gamma_{52–88}$KI (d).

Substitutions are underlined and in bold.

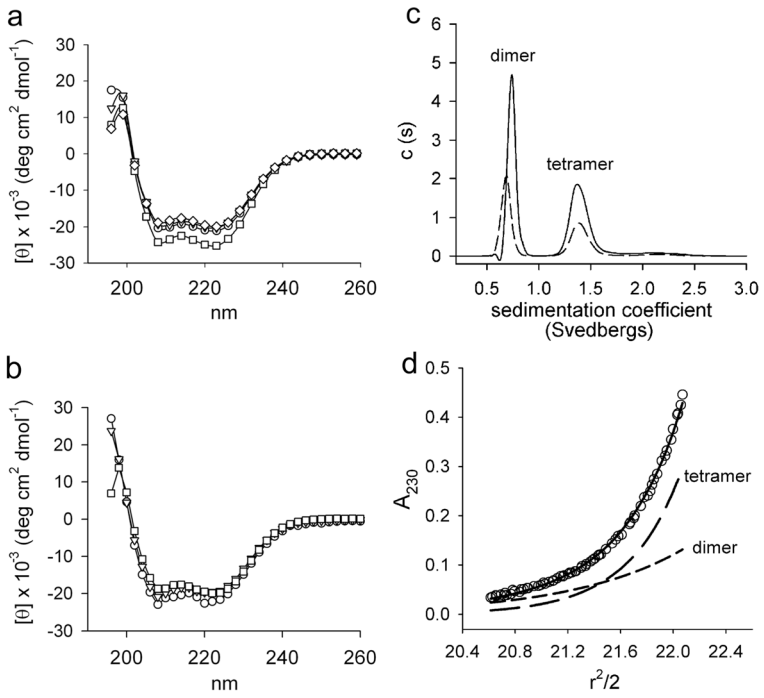

Figure 3.

Folding and oligomerization of peptide $\gamma_{52–88}$KI. (a) CD of $\gamma_{52–88}$KI, 100 μM, pH 4 (○), pH 5.5 (▽), pH 6.5 (□), pH 7 (◇) in PBS. (b) CD of 10 μM peptide (○), 20μM peptide (▽), 100 μM peptide (□) at pH 7 in PBS. (c) Sedimentation coefficient distribution for $\gamma_{52–88}$KI at 90μM (solid line) and 45 μM (dashed line) in PBS, as determined by AUC sedimentation velocity. (d) Representative AUC sedimentation equilibrium data for $\gamma_{52–88}$KI taken from a global analysis of six curves. Data shown is 45μM $\gamma_{52–88}$KI in PBS at 36,000 rpm. The solid line shows the fit to the data (○); dashed lines illustrate the relative proportion of dimer and tetramer species.

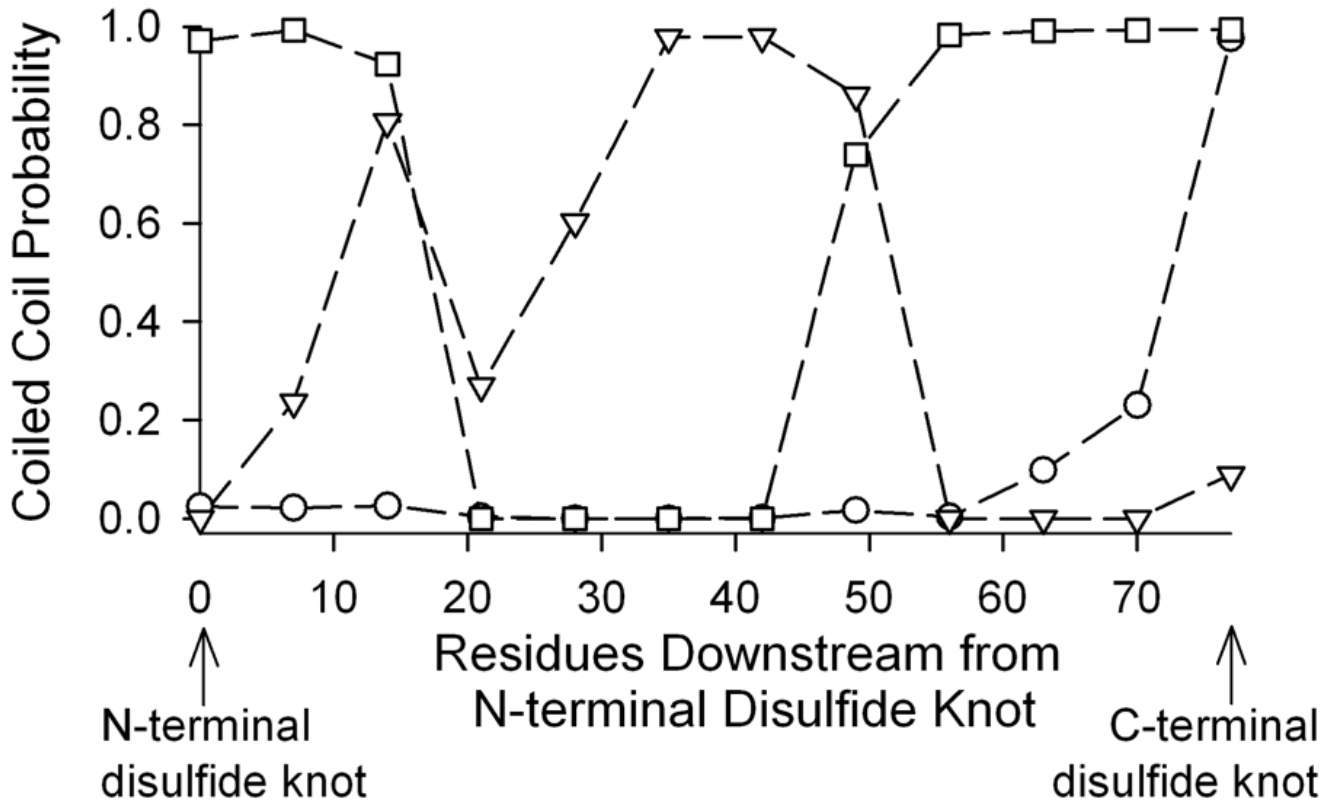

Figure 4.

Coiled coil prediction for an overlapping series of 35-amino acid peptides spanning the α-chain (○), β-chain (▽) and γ-chain (□) of the human fibrin coiled coil domain. The *x* axis represents the number of residues separating the N-terminal disulfide knot in fibrin and the first amino acid of each peptide; the last peptide in each series has a C-terminus coinciding with the C-terminal disulfide knot. Predictions made with MULTICOIL.[44]

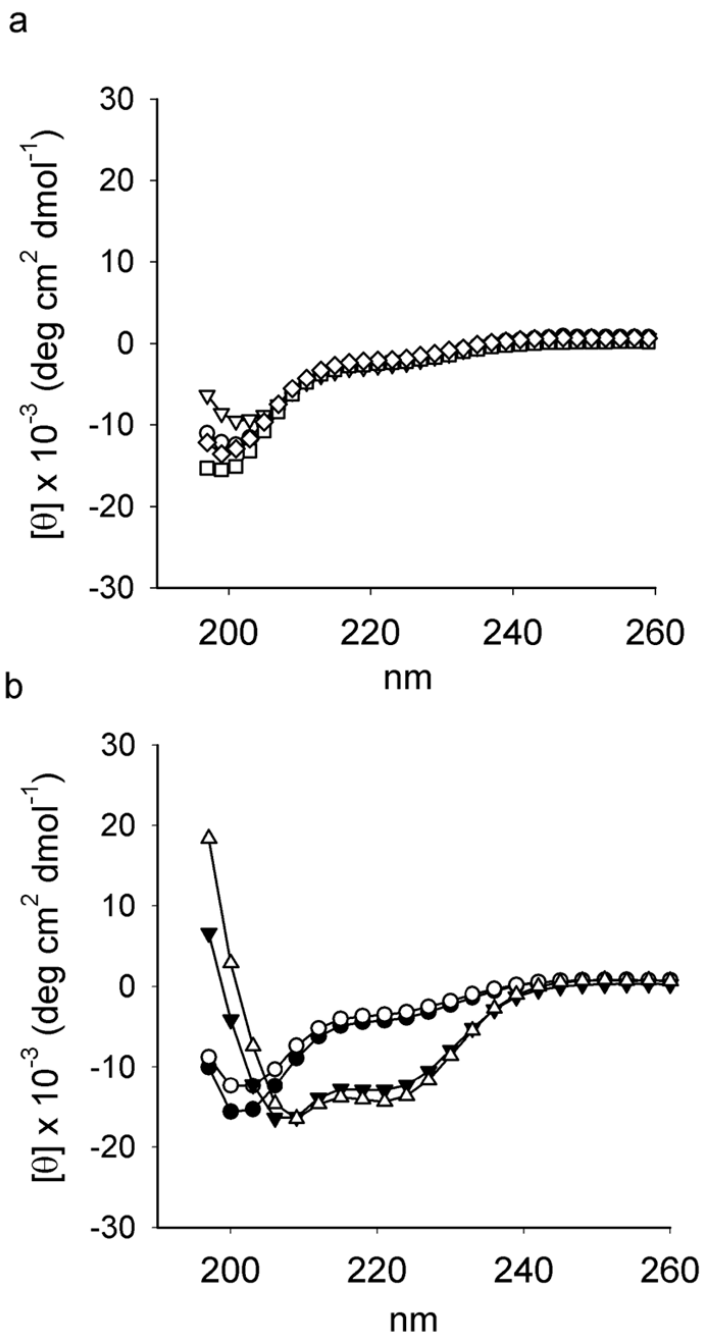

Figure 5.

Circular dichroism. (a) Native peptides$\alpha_{68–102}$ (▽), $\beta_{110–144}$ (□), $\gamma_{49–83}$ (◇), and the ternary mixture (○) at pH 7. (b) Peptide $\gamma_{49–83}$QQK (filled symbols) and $\gamma_{49–83}$ (open symbols) at pH 7 (●, ○) and pH 4.5 (▼, △). All measurements were taken at 100μM total peptide in PBS.

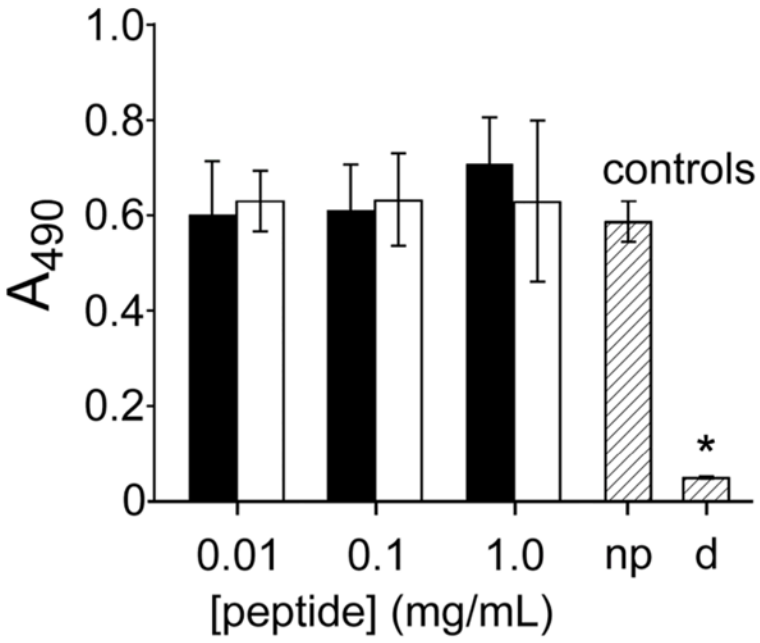

Figure 6.

Neither $\gamma_{49–83}$QQK (white bars) nor $\gamma_{52–88}$KI (black bars) was cytotoxic to human endothelial cells by MTS assay. Controls were cultures with no peptide (np) and dead cells (d). Means ± one standard deviation, *significantly lower viability than np by ANOVA with Tukey's HSD post-hoc test, n = 6, $p < 0.05$ considered significant.

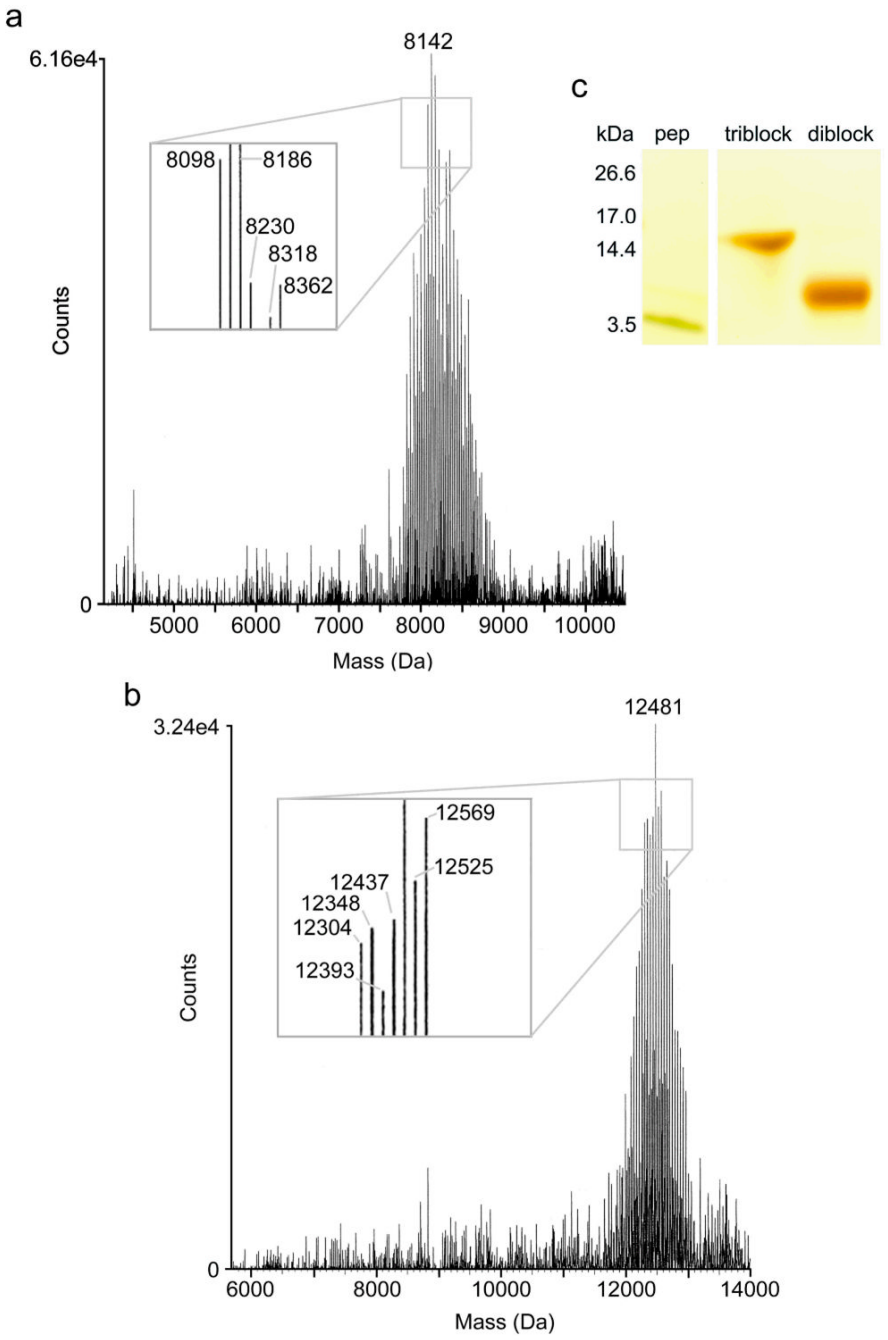

Figure 7.
ESI mass spectrometry of PEG-γKI (a) and γKI-PEG-γKI (b), and SDS-PAGE of γ_{52-88}KI, PEG-γKI, and γKI-PEG-γKI (c).

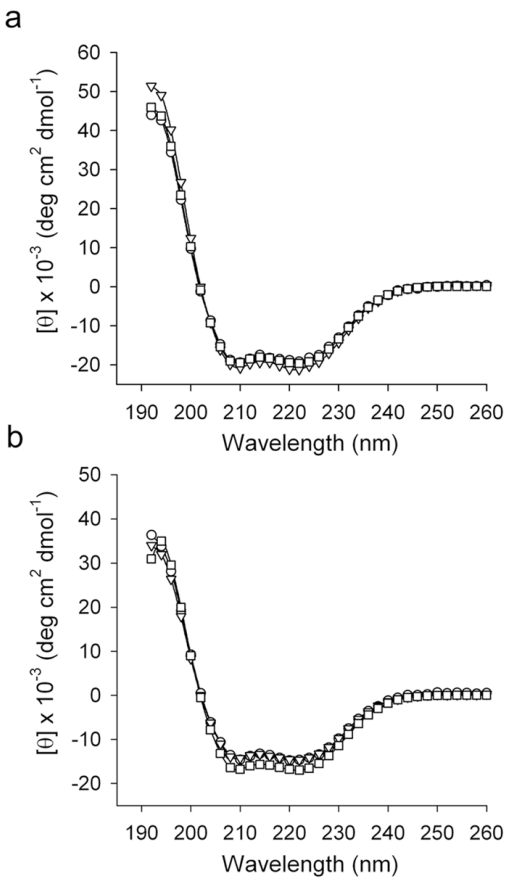

Figure 8.
Circular dichroism of PEG-γKI (a) and γKI-PEG-γKI (b), 10 μM (○), 20 μM (▽), and 100 μM (□). All samples measured in PBS, pH 7.4.

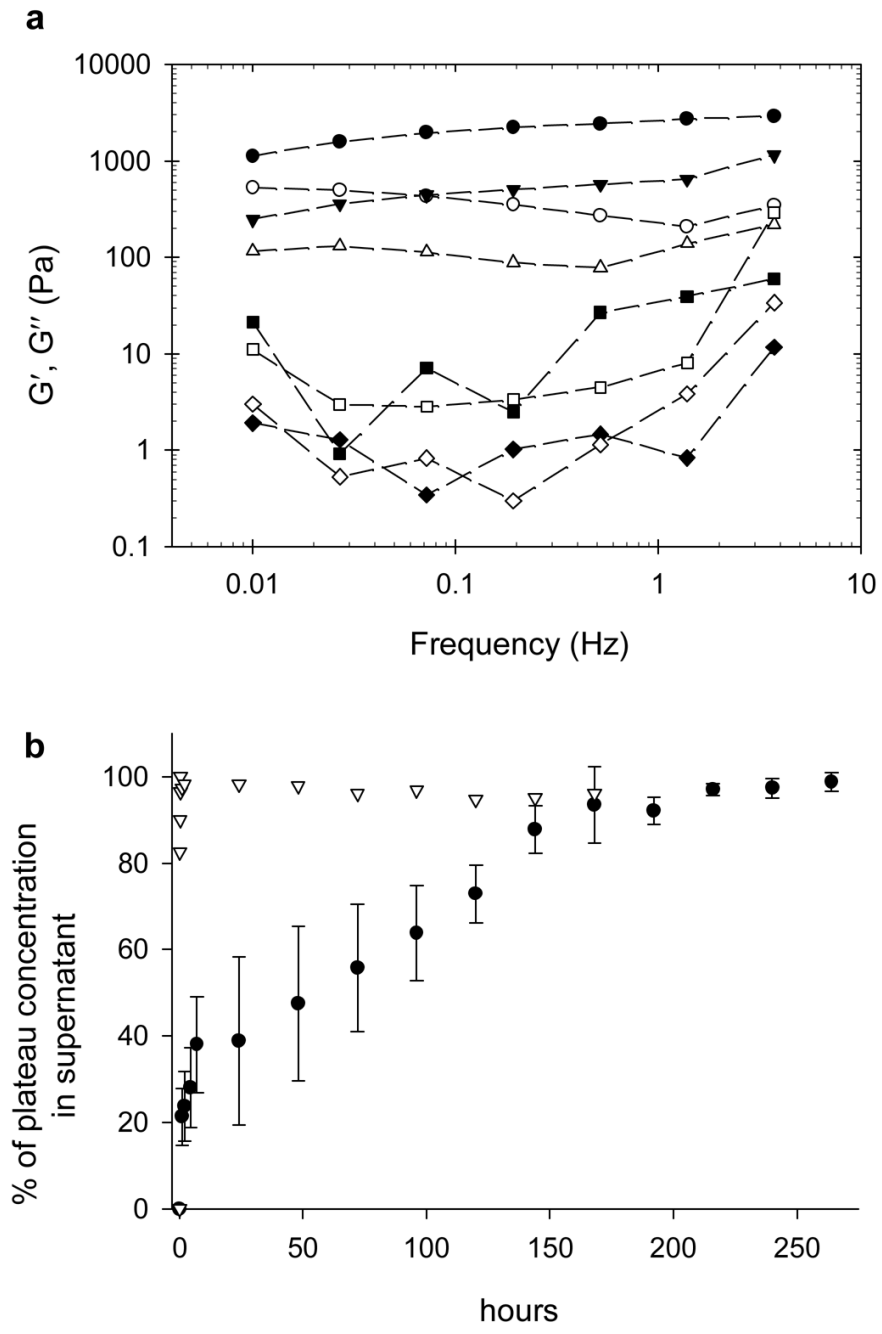

Figure 9.

Viscoelasticity (a) of 12 wt % γKI-PEG-γKI (G′ ●; G″ ○), 8 wt % γKI-PEGγKI (G′ ▼; G″ △), 12 wt % PEG-γKI (G′ ■, G″ □), and 8 wt % PEG-γKI (G′ υ, G″ ◇). Dissolution kinetics (b) of PEG-peptides from 8 wt% hydrogels. Diblock PEG-γKI (▽) and triblock γKI-PEG-γKI (●), n = 3, means ± standard deviation.

Table 1

Peptide helix positions, sequences, and substitutions (underlined).

Position:	**e**	**f**	**g**	**a**	**b**	**c**	**d**	**e**	**f**	**g**	**a**	**b**	**c**	**d**	**e**	**f**	**g**	**a**	**b**	**c**	**d**	**e**	**f**	**g**	**a**	**b**	**c**	**d**	**e**	**f**	**g**	**a**	**b**	**c**	**d**	**e**	**f**	**g**	**a**	**b**
$\alpha_{68–102}$	C	R	M	K	G	L	I	D	E	V	N	Q	D	F	T	N	R	I	N	K	L	K	N	S	L	F	E	Y	Q	K	N	N	K	D	S					
$\beta_{110–144}$	C	Q	L	Q	E	A	L	L	Q	Q	E	R	P	I	R	N	S	V	D	E	L	N	N	N	V	E	A	V	S	Q	T	S	S	S	S					
$\gamma_{49–83}$	C	G	I	A	D	F	L	S	T	Y	Q	T	K	V	D	K	D	L	Q	S	L	E	D	I	L	H	Q	V	E	N	K	T	S	E	V					
$\gamma_{49–83}$QQK	Q	Q	I	A	D	F	L	S	T	Y	Q	T	K	V	D	K	K	L	Q	S	L	E	D	I	L	H	Q	V	E	N	K	T	S	E	V					
$\gamma_{52–88}$KI				I	D	F	I	S	T	Y	I	T	K	I	D	K	K	I	Q	S	I	E	D	I	I	H	Q	I	E	N	K	I	S	E	I	K	Q	L	I	K

Table 2

Mean residue ellipticities of fibrin-inspired coiled coil peptides and peptide-polymers.[a]

Peptide	$[\theta]_{222} \times 10^{-3}$ (deg·cm^2·dmol^{-1})	$[\theta]_{222}/[\theta]_{208}$
$\alpha_{68–102}$	−2.6	0.39
$\beta_{110–144}$	−2.4	0.33
$\gamma_{49–83}$	−2.0	0.32
$\gamma_{49–83}$QQK[b]	−12.8	0.77
$\gamma_{52–88}$KI	−20.0	1.06
PEG-γKI (diblock)	−19.7	1.03
γKI-PEG-γKI (triblock)	−17.0	1.03

[a] 100μM peptide in PBS, pH 7 unless otherwise noted.

[b] pH 4.5